DOE/ER/76027-1

Analysis of Burnable Poison in Ford Nuclear Reactor Fuel to Extend Fuel Lifetime

Final Report for the Period
August 1, 1994 – September 29, 1996

Principal Investigators
Reed R. Burn
John C. Lee

Research Assistants
Luiz C. Faria
Jeffrey L. Voskuil
Amitava Majumdar

Nuclear Reactor Laboratory and
Department of Nuclear Engineering and Radiological Sciences
University of Michigan
Ann Arbor, Michigan 48109

December 1996

Prepared for

THE U. S. DEPARTMENT OF ENERGY
AGREEMENT NO. DE-FG02-94ER76027

Analysis of Burnable Poison in Ford Nuclear Reactor Fuel to Extend Fuel Lifetime

Abstract

The objective of the project was to establish the feasibility of extending the lifetime of fuel elements for the Ford Nuclear Reactor (FNR) by replacing current aluminide fuel with silicide fuel comprising a heavier uranium loading but with the same fissile enrichment of 19.5 wt. % ^{235}U. The project has focused on fuel designs where burnable absorbers, in the form of B_4C, are admixed with uranium silicide in fuel plates so that increases in the control reactivity requirements and peak power density, due to the heavier fuel loading, may be minimized. We have developed equilibrium cycle models simulating current full-size aluminide core configurations with 43~45 fuel elements. Adequacy of the overall equilibrium cycle approach has been verified through comparison with recent FNR experience in spent fuel discharge rates and simulation of reactor physics characteristics for two representative cycles. Fuel cycle studies have been performed to compare equilibrium cycle characteristics of silicide fuel designs, including burnable absorbers, with current aluminide fuel. These equilibrium cycle studies have established the feasibility of doubling the fuel element lifetime, with minimal perturbations to the control reactivity requirements and peak power density, by judicious additions of burnable absorbers to silicide fuel. Further study will be required to investigate a more practical silicide fuel design, which incorporates burnable absorbers in side plates of each fuel element rather than uniformly mixes them in fuel plates.

1. Introduction

The Ford Nuclear Reactor (FNR) at the University of Michigan is a swimming-pool type reactor utilizing MTR-type fuel elements with a rated power of 2 MW. Typical FNR core configurations comprise 42~45 uranium aluminide (UAl_x) fuel elements with a ^{235}U enrichment of 19.5 wt. %. Currently 8~9 standard fuel elements, containing 18 fuel plates each, and 2~3 control fuel elements, containing 9 plates each, are discharged annually and an equal number of new fuel elements are loaded into the core. We have performed a fuel cycle analysis and an initial fuel design analysis to assess the feasibility of replacing UAl_x fuel elements currently in use with uranium silicide (U_3Si_2) fuel elements comprising a higher uranium loading but with the same ^{235}U enrichment. The silicide fuel is expected to extend the lifetime of each fuel element and result in a substantial reduction in fuel cost.

In this study, we have developed an equilibrium cycle model for the FNR to investigate silicide fuel designs, with and without burnable absorbers. The equilibrium cycle model is based on previous studies[1,2] involving a combination of micro- and macro-cycles for the FNR core with 39 fuel elements, but reflects recent FNR configurations involving as many as 45 fuel elements. The 39-element equilibrium cycle model represents FNR core configurations of the late 1970s and early 1980s, when the conversion from high-enrichment uranium to low-enrichment uranium (LEU) fuel was undertaken. The FNR achieved an initial criticality with LEU fuel elements in late 1981, thereby providing a whole-core demonstration of LEU fuel designs. The 45-element core configuration is the largest feasible in a grid of (6×8) fuel locations, with allowances made for incore irradiation locations. We present in Figure 1 the overall layout of the FNR core, with the lattice positions for fuel elements indicated. Typically, lattice position L-5, L-67, and L-75 are not loaded with fuel to accommodate irradiation samples. We have endeavored to develop equilibrium cycle models for full-size core configurations that may accurately represent relevant core and reactivity characteristics of recent FNR cycles, including the burnup of discharged fuel elements and number of fuel elements discharged annually. The primary purpose of the present study was to compare, using realistic equilibrium cycle configurations, the performance of U_3Si_2 fuel designs and current UAl_x fuel.

Together with updating the core configuration, an effort was also made to improve the lattice analysis for individual fuel elements so that a more accurate set of macroscopic cross sections is used in global diffusion-depletion analysis. Thus, the WIMS-D4M collision probability code,[3] recently modified at Argonne National Laboratory (ANL), has replaced the LEOPARD unit-cell code[4] as our basic lattice physics tool. A more consistent geometrical representation of fuel plates has also been developed.

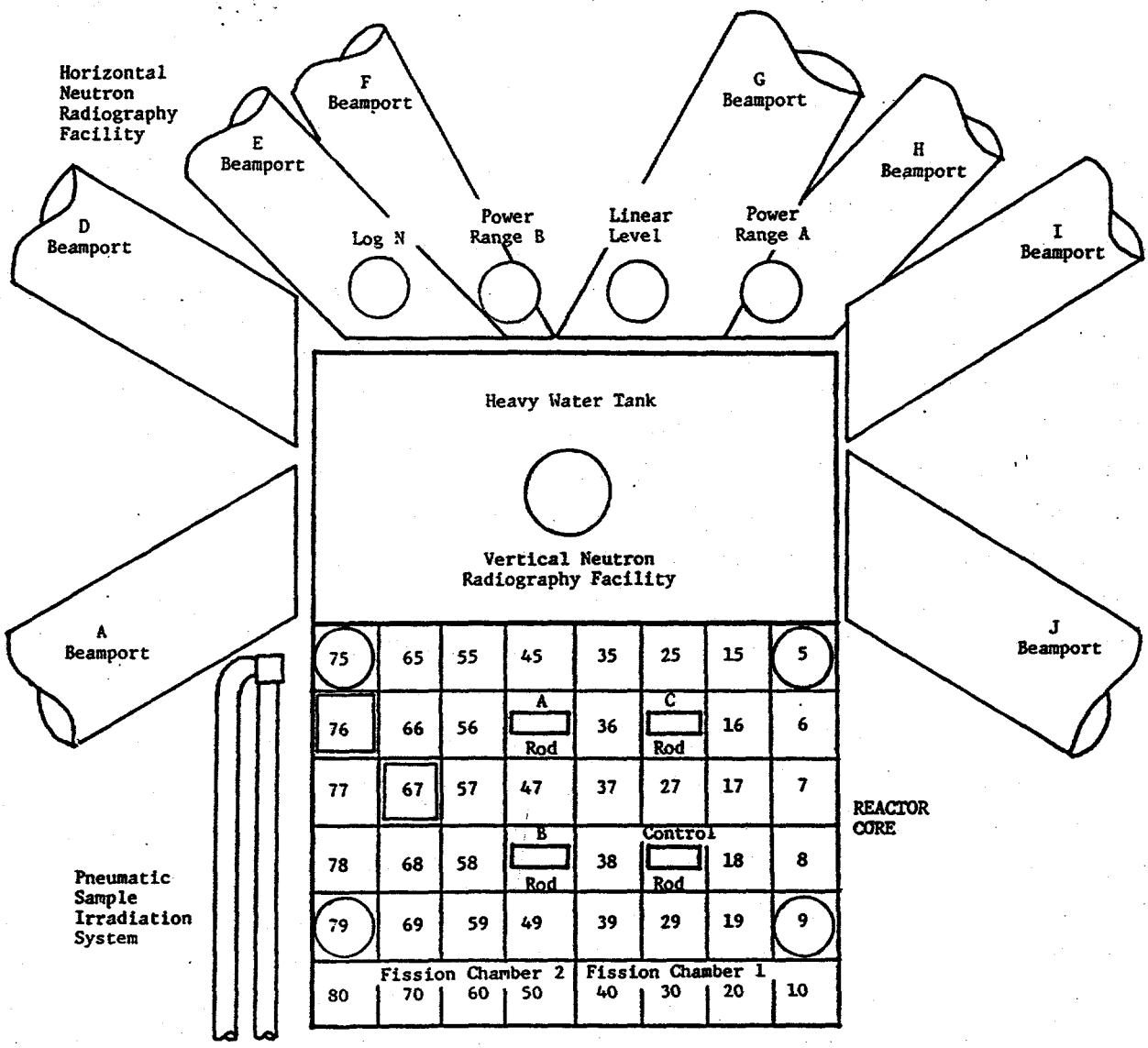

Figure 1. Ford Nuclear Reactor Core Layout

We present in Section 2 a brief description of the modifications we have made to the ANL version of WIMS and the revised geometrical model we have adopted for the one-dimensional representation of both the standard fuel element (SFE) and control fuel element (CFE). Section 3 discusses the fuel shuffling schemes we have developed for equilibrium core configurations comprising 43~45 elements. We compare the equilibrium cycle results for the aluminide and silicide designs in Section 4, followed by concluding remarks in Section 5.

2. WIMS Modeling of the FNR Fuel Elements

Before we began the task of developing full-size equilibrium cycle models for the FNR core, we had to modify the WIMS-D4M code so that the neutron leakage spectrum is used correctly to collapse multigroup cross sections into few-group macroscopic cross sections for the lattice and nonlattice regions separately. For this purpose, we introduce an approximation that the spatial flux distribution in each neutron energy group in a multigroup structure is unaffected by neutron leakage. Thus, we modulate the four-region, infinite-medium flux distributions, representing the fuel, clad, moderator and extra regions, by a multigroup leakage flux spectrum calculated for the entire fuel lattice. In Figure 2, we present schematics for the SFE and CFE lattices, together with the (6×6) heterogeneous mesh structures used to represent both fuel element types in global diffusion-depletion calculations. To handle the central water hole and 9 fuel plates explicitly for the CFE lattice, additional modifications were made to the WIMS-D4M code to tally lattice and nonlattice cross sections for the entire fuel element.

Together with these modifications to the WIMS-D4M code, we have also revised the geometrical modeling in the one-dimensional WIMS-D4M representation of fuel plates. One key change is to use the actual thickness for the fuel meat and clad regions in each fuel plate, rather than preserving the thickness of the water gap in our old LEOPARD setup.[1,2] In addition, the actual design specifications are used to arrive at a nominal surface area of fuel meat as an average between the maximum and minimum areas allowed. This yields a fuel meat length of 23.25" and a curved width of 2.32" or a straightened width of 2.3028". To accommodate the plate straightening and to preserve the material contents in the fuel and clad, number densities of fuel and clad materials are increased by the ratio 2.32/2.3028 = 1.007. Similarly, the number densities in the water gap are reduced to conserve the water mass but no adjustments are made to nonlattice number densities or volumes. These changes in the lattice and nonlattice geometrical representations are also reflected in a new mesh structure adopted in global diffusion theory calculations with the UM2DB code, which is a substantially modified version of the 2DB code.[5] In the WIMS model of the

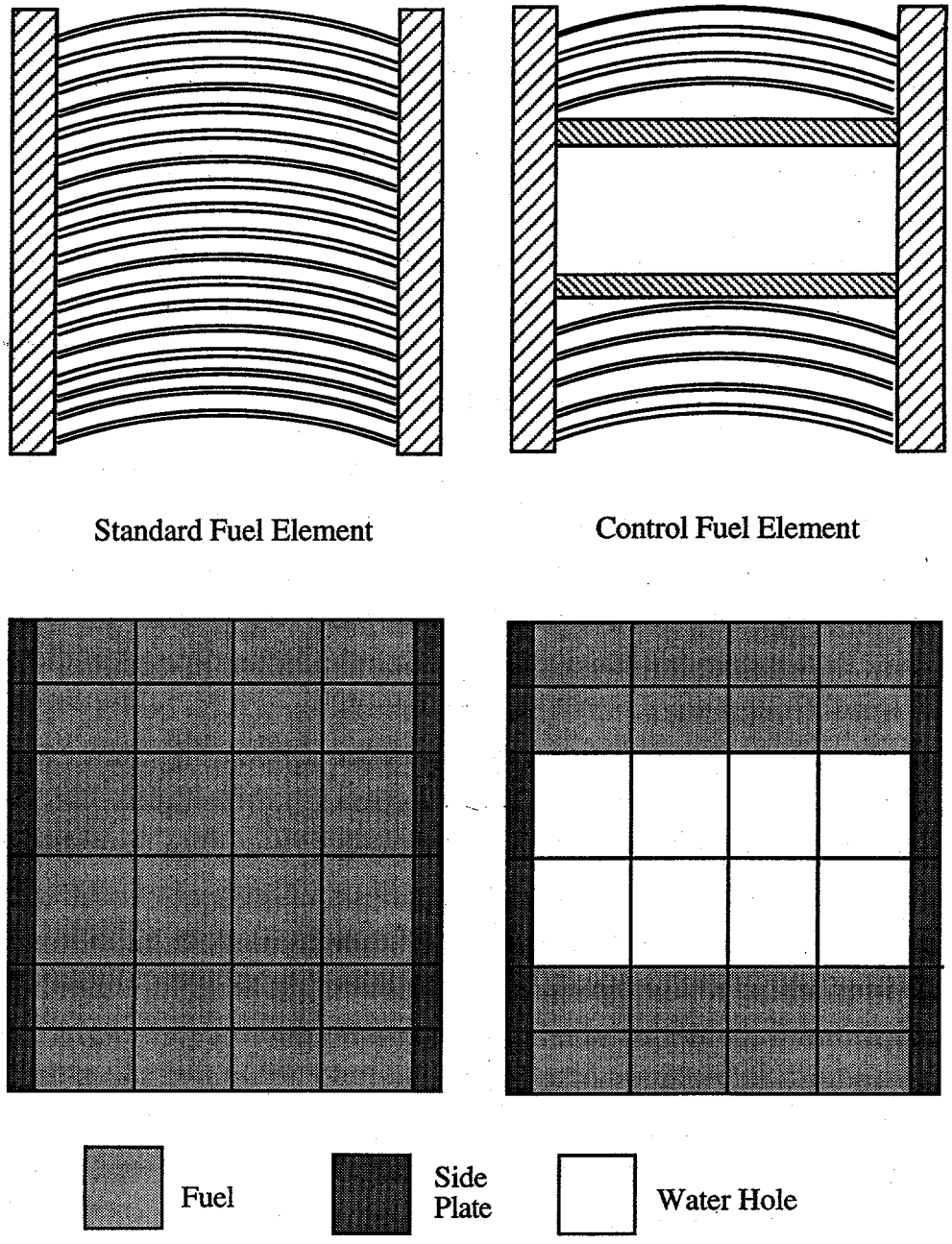

Figure 2. Standard and Control Fuel Element Layout

FNR fuel elements, trace quantities of various impurities, including ^{234}U and ^{236}U, are represented with the hot full power temperature of 160 °F for the fuel and clad, and 130 °F for the moderator and nonlattice regions. Thermal expansion in fuel and clad is not, however, represented in the number densities or the dimensions for the fuel and clad regions. Thus, the WIMS-generated macroscopic cross sections may be considered to represent mostly a hot zero power condition, with full effects of Doppler broadening included.

For the current equilibrium cycle study comparing aluminide and silicide fuel designs, we have limited ourselves to 60-mil fuel plate designs, with a meat thickness of 0.03" for the aluminide and 0.02" for the silicide fuel. Our study compares aluminide fuel elements comprising 0.167 kg ^{235}U per 18 plates with silicide elements comprising 0.225 kg ^{235}U. In the silicide design, two different loadings of burnable neutron absorbers in the form of B_4C are evaluated together with a design without burnable absorbers.

3. Equilibrium Cycle Model for the Full-Size Core

To summarize recent FNR fuel shuffling schemes, approximately 40 two-week cycles covering the period of October 1993 through May 1995 were analyzed. This analysis suggests that CFEs are used primarily in the four control locations surrounding the lattice position L-37 at the core center and that minor shuffles involving only SFEs are made over most of the cycles, followed by infrequent but major shuffles involving both SFEs and CFEs. The core size varied between 42 and 45 elements depending on the number of new fuel elements loaded.

These core configurations are idealized into a sequence of repetitive cycles involving three major shuffles and three minor shuffles each. This fuel shuffling scheme involves varying core sizes of 43~45 fuel elements, as summarized in Table I, and is labeled scheme A. We have also developed continuous shuffling schemes, labeled B and C, which involve nearly the same number of fuel movements per cycle, as summarized in Tables II and III, respectively. Shuffling schemes B and C both involve a fixed core size of 45 elements and are identical, except that different locations are used for the initial placements of some SFEs. Through these shuffling schemes, we may readily implement multiple fuel depletion steps for convergence to an equilibrium cycle configuration and may allow for more nearly constant core configurations than are attainable with recent FNR fuel shuffling schemes. In our fuel cycle study to date, Scheme A has been used for the aluminide design, while schemes B and C have been used both for the aluminide and silicide designs.

Table I. Fuel Shuffling Scheme for a (43-45)-Element Aluminide Core – Scheme A

Micro-cycle	Number of Elements	Fresh Fuel	Fuel Shuffling	Storage
1A	44	SFE SFE	F→37→47→25→56→07→65→69→80→D F→36→27→45→58→08→68→70→79→D 06→E	80→S_1
1B	45		S_1→06	
2A	43	SFE SFE CFE	F→38→57→49→15→40→09→77→79→D F→37→17→29→19→30→66→76→D F→26→46→48→28→D 06→E 80→E	06→S_2
2B	44		S_2→06	
3A	43	SFE SFE	F→36→35→16→55→50→60→10→06→D F→38→39→18→59→20→78→D 79→E	06→S_2 78→S_3
3B	45		S_2→80 S_3→79	

F = fresh fuel loaded, D = fuel discharged, E = fuel discharged and left empty, S_n = fuel in storage

Table II. Fuel Shuffling Scheme for the 45-Element Silicide Core – Scheme B

Microcycle	Fresh Fuel	Fuel Shuffling
1	SFE CFE	F→37→47→25→56→07→65→69→79→D F→26→48→46→28→D
2	SFE	F→36→27→45→58→08→68→70→06→D
3	SFE	F→38→57→49→15→40→09→77→80→D
4	SFE CFE	F→37→17→29→19→30→66→76→79→D F→26→48→46→28→D
5	SFE	F→36→35→16→55→50→60→10→06→D
6	SFE	F→38→39→18→59→20→78→80→D

Table III. Fuel Shuffling Scheme for the 45-Element Silicide Core – Scheme C

Microcycle	Fresh Fuel	Fuel Shuffling
1	SFE CFE	F→47→37→25→56→07→65→69→79→D F→26→46→48→28→D
2	SFE	F→27→36→45→58→08→68→70→06→D
3	SFE	F→38→57→49→15→40→09→77→80→D
4	SFE CFE	F→47→17→29→19→30→66→76→79→D F→26→46→48→28→D
5	SFE	F→27→35→16→55→50→60→10→06→D
6	SFE	F→38→39→18→59→20→78→80→D

Our equilibrium cycle models are similar to a 39-element shuffling scheme developed as part of the original LEU fuel design[1,2] and consider six microcycles making up a macrocycle with eight fuel loading zones for SFEs and four zones for CFEs for a total of 45 fuel elements. The lattice positions in each SFE loading zone are selected to have nearly the same power fractions so that SFEs are moved sequentially through positions of decreasing power fraction while CFEs are simply moved through the four control lattice positions sequentially. Among the eight SFE zones, for schemes B and C, zones 1 and 8 comprise three lattice positions each so that zone 1 accommodates new elements and zone 8 discharges depleted elements with a period of three microcycles. The remaining SFE zones have six lattice positions each, with the exception of zone 5 which has only five positions to accommodate incore irradiations at lattice position L-67. As detailed in Tables II and III, one fresh SFE, marked *F*, is loaded and one depleted SFE, designated *D*, is discharged each microcycle, while one CFE is loaded and discharged every third microcycle.

In fuel shuffling scheme A, to minimize the frequency of major shuffles, new fuel elements are loaded every other microcycle, accompanied by minor shuffles at the intervening microcycles. Thus, at each major shuffle in microcycles 1A, 2A, and 3A, two SFEs are loaded, with the loading patterns of scheme B, combined with one CFE loaded only at microcycle 2A. The minor shuffles involve reloading SFEs from storage locations, marked S_n, $n = 1, 2, 3$. Only one new CFE is loaded per macrocycle in scheme A, compared with two new CFEs loaded in schemes B and C. In addition, to accommodate variable core sizes ranging between 43 and 45 elements, microcycles 1A, 2A and 3A also involve discharging fuel elements, leaving empty some lattice positions, marked *E*. Thus, scheme A is a variation of scheme B, entailing a double loading of SFEs at microcycles 1A, 2A, and 3A, which in turn requires reducing the core size at these microcycles to minimize uneven reactivity swings over microcycles. Scheme A simulates current FNR loading patterns closely and reflects the operational objective that major shuffling frequencies be minimized. This is a desirable objective because shim-safety rod calibrations, involving extra time and effort, are required at major shuffles but not at minor shuffles.

All of our UM2DB fuel depletion calculations have been performed with a (6×6) heterogeneous mesh, with the lattice and nonlattice regions represented distinctly by separate sets of burnup-dependent cross sections as illustrated in Figure 2. In our current equilibrium cycle study, fuel depletion is calculated without any explicit consideration of partial insertion of shim-safety or regulating rods into the core during a fuel cycle. Furthermore, no effort has been made so far to calculate the control rod worths or estimate the shutdown reactivity margin in an equilibrium core; further study will have to involve these reactivity related calculations in detail.

The actual approach to an equilibrium core configuration was modeled by iteratively varying the cycle length until the reactivity swings over successive macrocycles converge to an asymptotic value and the end-of-cycle (EOC) reactivity requirements are satisfied. Based on WIMS/UM2DB simulations of two recent FNR configurations, Cycles 349A and 380B, we assume a reactivity bias of 1.3~1.6 $\%\Delta k/k$. Together with a minimum reactivity allowance of 0.5 $\%\Delta k/k$ for experiments at EOC, our iterative search for an equilibrium cycle length is terminated when the core reactivity at EOC of the sixth microcycle, in a converged macrocycle, reaches a value of 1.8~2.1 $\%\Delta k/k$, or preferably 2.0 $\%\Delta k/k$. Both for the aluminide and silicide fuel designs, increasing the cycle length results in a higher core-average fuel burnup for the equilibrium cycle and decreases the EOC core eigenvalue.

4. Equilibrium Cycle Results for the Aluminide and Silicide Cores

Using the shuffling schemes presented in Tables I through III and the EOC reactivity requirements considered in Section 3, we performed batches of UM2DB calculations comprising 12 macrocycles, for a total of 72 microcycles, both for the aluminide and silicide cores. We illustrate in Figure 3 the evolution of the UM2DB effective multiplication factor k_{eff}, corresponding to equilibrium xenon concentrations, during the last six macrocycles for the aluminide and silicide reference cases A-5 and S-4, which will be discussed later. Macrocycles 11 and 12 show nearly asymptotic reactivity behavior for each case and equilibrium cycle characteristics are calculated through an average over six microcycles of macrocycle 12. For computational convenience, however, the core average burnup, thermal flux, and power peaking factor F_{xy} are calculated at a particular microcycle in macrocycle 12, when the largest peaking factor is encountered. As a measure of the overall reactivity control requirements, we determine the total reactivity swing over a macrocycle, rather than the reactivity changes averaged over microcycles.

Table IV summarizes equilibrium cycle characteristics for the aluminide fuel, where we compare the full-size core results with 39-element calculations based on our current WIMS/UM2DB setup as well as the WIMS/REBUS system[6] and LEOPARD/UM2DB setup.[2] The differences between cases A-1 and A-2 are due to differences in the lattice physics codes used as well as in the spatial mesh structure for the UM2DB calculations. The differences between cases A-2 and A-3 primarily reflect differences in the bases or definitions for the reactivity change rates.

Comparison of cases A-2 and A-5 in Table IV indicates that the cycle length is essentially doubled from 16.5 equivalent full power days (EFPDs) to 32.8 EFPDs by increasing the core size from 39 to 45 elements and by loading two less CFEs in the core. We also note that the core average burnup at the beginning of cycle (BOC) and the average

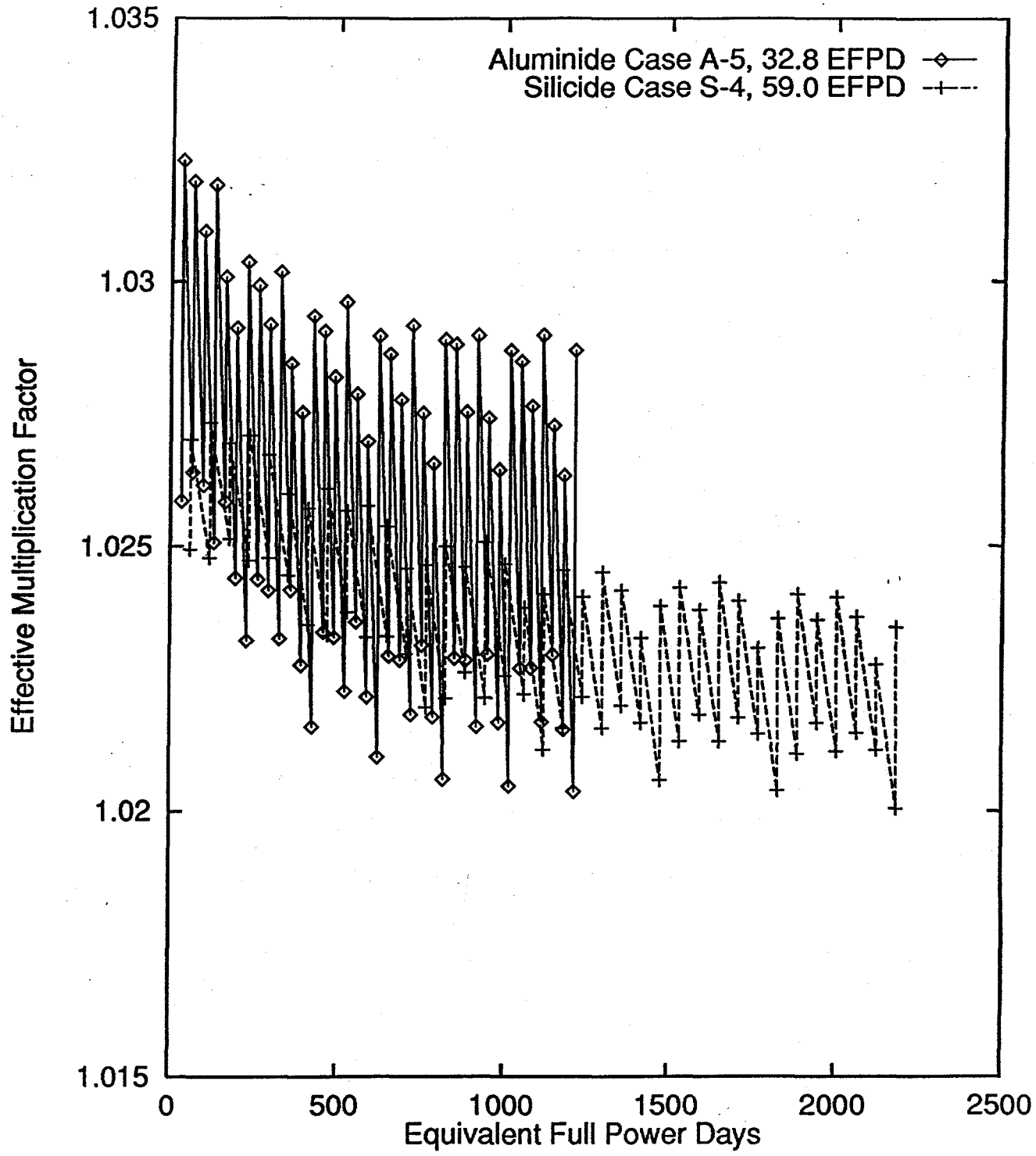

Figure 3. Effective multiplication factor during the approach to equilibrium cycle

Table IV. Equilibrium Cycle Characteristics for the Aluminide Core

Case number	A-1	A-2	A-3	A-4	A-5
Number of fuel elements	39	39	39	43~45	45
Cycle length (EFPD)	16.5	16.5	16.5	30.0	32.8
Fuel shuffling scheme	---	---	---	A	B
Method of analysis (Lattice physics/global)	LEOPARD UM2DB*	WIMS UM2DB	WIMS REBUS+	WIMS UM2DB	WIMS UM2DB
Reactivity change over macrocycle($\%\Delta k/k$)	–0.31	–0.33	–0.51+	–0.81	–0.84
Reactivity change rate ($\%\Delta k/k$ per EFPD)	–0.019	–0.018	–0.031+	–0.018	–0.017
Core average burnup at BOC (% initial ^{235}U)	11.1	10.4	11.7	20.2	22.5
Average discharge burnup (% initial ^{235}U)	19.1	SFE: 19.5 CFE: 17.4	20.6	SFE: 36.9 CFE: 38.9	SFE: 40.2 CFE: 23.1
Core average power density (MW/m^3)	13.8	13.8	13.8	11.9~12.5	11.9
Core average thermal flux ($10^{13} n/cm^2 \cdot s$)	1.15	1.03	1.11	1.03	1.01
Power peaking factor F_{xy}	1.70	1.92	—	2.14	2.27
Effective multiplication factor at end of macrocycle	—	1.0337	1.0298	1.0203	1.0204
Number of fuel elements discharged per year	SFE: 15.8 CFE: 5.3	SFE: 15.8 CFE: 5.3	SFE: 15.8 CFE: 5.3	SFE: 8.7 CFE: 1.5	SFE: 8.0 CFE: 2.7

* UM2DB calculations with (2×2) homogeneous mesh per fuel element, Ref. 2
\+ Ref. 6

burnup of discharged fuel elements both increase significantly. This results in essentially halving the number of fresh fuel elements required and the number of depleted fuel elements to be discharged and disposed of. The calculated discharge burnups of 40% and 23% of initial ^{235}U for SFEs and CFEs, respectively, for case A-5 compare favorably with the recent FNR experience of 38% and 21%. Similarly, the number of fuel elements discharged annually, 8.0 SFEs and 2.7 CFEs, closely approximates FNR experience over the past six years: 8.3 SFEs and 2.0 CFEs discharged annually. Due to the use of one less CFE per macrocycle, case A-4 yields a cycle length of 30.0 EFPDs, which is 9% smaller than that for case A-5, with the corresponding differences in fuel burnup distributions and fuel discharge rates.

Using the (6×6) heterogeneous mesh structure in our UM2DB calculations, we also obtain the radial peaking factor $F_{xy} = 2.17$ for cycle 349A and $F_{xy} = 1.99$ for cycle 380B, which compare favorably with $F_{xy} = 2.14$ and 2.27 calculated for cases A-4 and A-5, respectively. Here, the peaking factor F_{xy} is defined as the ratio of the peak power density to the power density averaged over the lattice regions of the core. Thus our equilibrium

cycle configurations, cases A-4 and A-5, appear to simulate, to an acceptable level, power distributions, fuel depletion rates, and reactivity characteristics of recent FNR core configurations. Fuel shuffling scheme A reflects more closely the recent FNR shuffling strategy, although case A-5, with shuffling scheme B, shows somewhat better agreement with the FNR fuel burnup data. Thus, we consider case A-4 our reference equilibrium aluminide configuration.

The difference in F_{xy} between cycles 349A and 380B indicates the sensitivity of the power peaking factor to actual fuel loading pattern. The main difference between the two recent FNR cycles is that two CFEs in the control locations are essentially new in cycle 349A, while all CFEs are substantially depleted in cycle 380B. Likewise, the difference in F_{xy} between cases A-4 and A-5 is primarily due to the differences in the fuel shuffling scheme. Although shuffling scheme A for case A-4 entails a doubling loading of SFEs at each major shuffle, when the worst power peak, corresponding to $F_{xy} = 2.14$, is encountered, one less SFE has been loaded up to that point in the macrocycle compared with case A-5. For case A-5, the worst power peak, corresponding to $F_{xy} = 2.27$, occurs at a later point in the macrocycle when a full load of new SFEs has taken place.

We should note that no explicit considerations were given to the EOC reactivity requirements and the calculated eigenvalue biases in the 39-element equilibrium cycle calculations summarized in Table IV. This has resulted in underestimating the cycle length of this smaller aluminide core that has served as a reference for earlier silicide fuel studies.[2,7]

Although we observe substantial increases in the cycle length and core average burnup for larger cores, the reactivity changes per EFPD of operation tend to remain nearly constant. This results in a substantial increase in magnitude of the reactivity swing over a macrocycle, which is somewhat larger than that expected by the increases in the cycle length. Although case A-4 uses shuffling scheme A entailing a double loading of SFEs at infrequent intervals, through variable core sizes, the reactivity swing of 0.81 $\%\Delta k/k$ over a macrocycle is kept slightly below that achievable with the more continuous and gradual shuffling scheme B utilized in case A-5 with a fixed core size of 45 elements. Although no explicit shutdown margin calculations have been performed, we believe the reactivity swing of 0.83 $\%\Delta k/k$ for the 30-EFPD cycle in case A-4 can be accommodated with the newly installed shim-safety rods comprising an alloy of titanium diboride (TiB_2) and aluminum.

We present a similar summary of equilibrium cycle characteristics for the silicide fuel in Table V. All of the cases summarized in Table V have been calculated with the WIMS and UM2DB codes for a fuel plate thickness of 0.06". All of the silicide cases show that, with a heavier fuel loading, silicide fuel provides significant increases in fuel utilization, as

Table V. Equilibrium Cycle Characteristics for the Silicide Core

Case number	S-1	S-2	S-3	S-4
Number of fuel elements	39	45	45	45
B_4C loading per plate (mg)	0.0	0.0	60.2	90.3
Cycle length (EFPD)	65.0	73.0	65.0	59.0
Fuel shuffling scheme	---	B	C	C
Reactivity change over macrocycle($\%\Delta k/k$)	–1.12	–1.65	–0.78	–0.39
Reactivity change rate ($\%\Delta k/k$ per EFPD)	–0.016	–0.015	–0.008	–0.004
Core average burnup at BOC (% initial ^{235}U)	31.6	38.0	33.0	29.6
Average discharge burnup (% initial ^{235}U)	SFE: 54.9 CFE: 51.5	SFE: 63.1 CFE: 41.8	SFE: 56.5 CFE: 35.2	SFE: 51.9 CFE: 30.8
Core average power density (MW/m^3)	13.8	11.9	11.9	11.9
Core average thermal flux ($10^{13}n/cm^2 \cdot s$)	1.02	0.92	0.96	0.84
Power peaking factor F_{xy}	2.42	2.69	2.37	2.20
Effective multiplication factor at end of macrocycle	1.0187	1.0200	1.0201	1.0201
Number of fuel elements discharged per year	SFE: 4.0 CFE: 1.3	SFE: 3.6 CFE: 1.2	SFE: 4.0 CFE: 1.3	SFE: 4.4 CFE: 1.5

* Fuel shuffling scheme slightly modified from scheme C

measured by the cycle length and fuel discharge rates. The reactivity change per EFPD tends to remain nearly independent of cycle length and core average burnup as is the case for the aluminide fuel. The reactivity change rates become, however, significantly smaller with borated silicide fuel, since the decrease in reactivity due to fuel depletion is compensated for by the concurrent depletion of B_4C. For a core average burnup corresponding to the equilibrium core of a given size and without burnable absorbers, the average amount of ^{235}U remaining in the core is nearly the same for the UAl_x and U_3Si_2 fuel. Due to a long fuel cycle, however, silicide case S-2, without burnable absorbers, shows a large reactivity swing on the order of 1.7 $\%\Delta k/k$ over a macrocycle.

In addition, comparison of Tables IV and V reveals a large increase in the radial power peaking factor F_{xy} for the equilibrium silicide core without burnable absorbers, e.g., case S-2 yields $F_{xy} = 2.69$. We note that the peak power density is usually observed in CFEs and that in general silicide configurations yield larger values of F_{xy} than aluminide cores. This is because the difference between the ^{235}U mass in a fresh fuel element loaded into the central region of the core and the average ^{235}U inventory in surrounding fuel elements is larger for an equilibrium silicide core than the corresponding aluminide core.

In an effort to constrain the reactivity swing that has to be accommodated by the shim-safety rods and to minimize the increase in the peaking factor F_{xy}, we have considered two different loadings of B_4C, admixed with fuel material in cases S-3 and S-4. With a loading of 60.2 mg B_4C per fuel plate, which is equivalent to a burnable absorber concentration of 0.094 wt. % of fuel, the reactivity swing over a macrocycle is dramatically reduced to a level comparable to that of the aluminide reference case A-4. In case S-3, shuffling scheme C is used instead of scheme B to achieve a maximum reduction in F_{xy}. Given the encouraging results for case S-3, a further increase in the burnable absorber loading to 90.3 mg per plate, or 0.14 wt. % of fuel, is considered in case S-4 to reduce the power peaking factor also to a level comparable to that of case A-4.

We note that we incur a slight increase in the power peaking factor from $F_{xy} = 2.14$ for the aluminide reference case A-4 to $F_{xy} = 2.20$ for the silicide case S-4, while the cycle length is essentially doubled from 30.0 EFPDs in case A-4 to 59.0 EFPDs in case S-4. In light of the fact that F_{xy} calculated for actual FNR configurations yields values up to 2.17 for cycle 349A, we may conclude that $F_{xy} = 2.20$ for case S-4 is essentially equal to the radial peaking factors expected in aluminide cores. Thus, case S-4 may be considered a reference silicide design essentially doubling the cycle length of the reference aluminide case A-4, without increasing the peak power density. Alternate fuel shuffling schemes similar to scheme A for the aluminide fuel have not been pursued for the silicide fuel since, with the cycle length doubled, major fuel shuffles will be required approximately at the same EFPD intervals for the silicide case S-4 as for the aluminide case A-4.

A fine tuning of the burnable absorber loading and other parameters, as well as a fuel shuffling scheme similar to scheme A involving a reduced number of CFEs loaded and discharged per macrocycle, may accomplish a further reduction in the power peaking factor for the silicide design. Such a detailed optimization study, however, has not been undertaken, because of the difficulty involved in ensuring a uniform admixing of B_4C and U_3Si_2 in the fuel plate manufacturing process. One possible way to overcome this difficulty is to load B_4C in the aluminum side plates and to have them assembled into fuel elements together with silicide fuel plates without burnable absorber loading. We are currently investigating ways to represent borated aluminum side plates in the one-dimensional WIMS modeling of both SFE and CFE lattices. Once an adequate WIMS model is developed, equilibrium fuel cycle studies will be performed for this alternate silicide fuel design. The present study has, however, established the feasibility of using silicide fuel with a heavier uranium loading in the FNR core such that the lifetime of fuel elements can be doubled with minimal perturbations to the operating strategy and core characteristics.

5. Concluding Remarks

We have developed equilibrium cycle models for full-size FNR core configurations, simulating recent FNR cycles with 43~45 fuel elements, and have used the models to perform preliminary comparisons of aluminide and silicide core characteristics. The equilibrium cycle results for the aluminide fuel compare favorably with recent FNR experience in terms of reactivity and fuel burnup characteristics, and fuel element discharge rates. The radial power peaking factor for the equilibrium aluminide core also shows close agreement with that for two recent FNR core configurations, cycles 349A and 380B. With a larger core and replacement of two CFEs by SFEs in non-control lattice locations, the cycle length for the aluminide equilibrium cycle with 43~45 elements is nearly double that for a 39-element aluminide cycle previously considered. For the silicide fuel, without burnable absorbers, case S-2 with a fixed core size of 45 elements yields a cycle length of 73.0 EFPDs, which is only 13% larger than that for the 39-element core, case S-1.

The cycle length for case S-2 is, however, 2.2 times that for the aluminide core of the same size, case A-5, and fuel element discharge rates decrease by the same factor, confirming the desirability of using silicide fuel, with a heavier fuel loading, in the FNR core. We note, however, that the radial peaking factor F_{xy} is considerably larger for a silicide core, with a heavier ^{235}U loading in fresh fuel elements surrounded by depleted fuel elements, whose average ^{235}U loading may be nearly the same as that of the corresponding aluminide core. In addition, the reactivity swing over a macrocycle is significantly increased in silicide core configurations without burnable absorbers.

This has prompted us to consider the possibility of admixing B_4C with uranium silicide in fuel plates. Equilibrium cycle studies with borated silicide fuel elements indicate the feasibility of essentially doubling the lifetime of fuel elements with minimal perturbations to the core power distributions and reactivity control requirements. Additional effort will be required to study the feasibility of loading B_4C in side plates of silicide fuel elements and to evaluate various fuel cycle characteristics for the alternate silicide fuel designs. Monte Carlo calculations are currently underway to develop a one-dimensional WIMS model that could represent B_4C-loaded side plates as part of the nonlattice region. Transition to an equilibrium silicide core from an equilibrium aluminide core should also be studied further with due considerations given for the results obtained by M. Bretscher.[6]

References

1. W. Kerr, J. S. King, J. C. Lee, W. R. Martin, and D. K. Wehe, "The Ford Nuclear Reactor Demonstration Project for the Evaluation and Analysis of Low Enrichment Fuel," ANL/RERTR/TM-17, Argonne National Laboratory (1991).

2. W. R. Martin, H. Nakata, T. C. Wan, J. Vujic, and J. C. Lee, "Analysis of Uranium Silicide Fuel for the Ford Nuclear Reactor," Proc. International Meeting on Reduced Enrichment for Research and Test Reactors, Gatlinburg, Tennessee (1986).

3. J. R. Deen, W. L. Woodruff, and C. I. Costescu, "WIMS-D4M User's Manual," ANL/RERTR/TM-23, Argonne National Laboratory (1995).

4. R. F. Barry, " LEOPARD – A spectrum Dependent Non-Spatial Depletion Code," WCAP-3269-26, Westinghouse Electric Corporation (1963).

5. W. W. Little Jr. and R. W. Hardie, "2DB User's Manual – Revision I," BNWL-831, REV1, Battelle Pacific Northwest Laboratory (1969).

6. M. M. Bretscher, J. L. Snelgrove, R. R. Burn, and J. C. Lee, "Use of Silicide Fuel in the Ford Nuclear Reactor to Lengthen Fuel Element Lifetimes," Proc. International Meeting on Reduced Enrichment for Research and Test Reactors, Paris (1995).

7. Private communication to J. C. Lee from M. M. Bretscher, August 17, 1994.